Nanotoxicology, 2010; Early Online, 1–14

Cerium oxide nanoparticle-induced pulmonary inflammation and alveolar macrophage functional change in rats

JANE Y. MA[1], HONGWEN ZHAO[2], ROBERT R. MERCER[1], MARK BARGER[1], MURALI RAO[1], TERENCE MEIGHAN[1], DIANE SCHWEGLER-BERRY[1], VINCENT CASTRANOVA[1], & JOSEPH K. MA[3]

[1]*Health Effects Laboratory Division, National Institute for Occupational Safety and Health, Morgantown, West Virginia,* [2]*Institute of Respiratory Diseases, The First Affiliated Hospital, China Medical University, Shenyang, P. R. China, and* [3]*School of Pharmacy, West Virginia University, Morgantown, West Virginia, USA*

(Received 19 November 2009; accepted 26 August 2010)

Abstract

The use of cerium compounds as diesel fuel catalyst results in the emission of cerium oxide nanoparticles (CeO_2) in the exhaust. This study characterized the potential effects of CeO_2 exposure on lung toxicity. Male Sprague Dawley rats were exposed to CeO_2 by a single intratracheal instillation at 0.15, 0.5, 1, 3.5 or 7 mg/kg body weight. At 1 day after exposure, CeO_2 significantly reduced NO production, but increased IL-12 production, by alveolar macrophages (AM) in response to *ex vivo* lipopolysacchride (LPS) challenge, and caused AM apoptosis, through activation of caspases 9 and 3. CeO_2 exposure markedly increased suppressor of cytokine signaling-1 at 1-day and elevated arginase-1 at 28-day post exposure in lung cells, while osteopontin was significantly elevated in lung tissue at both time points. CeO_2 induced inflammation, cytotoxicity, air/blood barrier damage, and phospholipidosis with enlarged AM. Thus, CeO_2 induced lung inflammation and injury in lungs which may lead to fibrosis.

Keywords: *Cerium oxide, nanoparticle, lung injury, alveolar macrophages, pulmonary fibrosis*

Introduction

High levels of diesel exhaust particles (DEP), in the environment or at workplaces, have been proposed to be a significant contributor to the development of acute and chronic lung diseases, including respiratory infection and allergic asthma (Yin et al. 2004; Dong et al. 2005). Cerium compounds, including cerium oxide, have been used as diesel fuel catalysts to enhance combustion by lowering the ignition temperature of the carbonaceous DEP; thereby, reducing the emission of particulate matter (PM) in diesel exhaust. A number of emission tests have shown that the cerium technology reduces substantially PM emissions and their organic content, but generates cerium oxide nanoparticles (CeO_2) in the diesel exhaust (Heeb 1998; Czerwinski et al. 2000).

The health effects of CeO_2 are not well understood. Studies have shown that inhaled CeO_2 induces both pulmonary and systemic toxicity in rats, including lung discoloration, enlargement of lymph nodes, increased lung weight, and dose-dependent increases in segmental blood neutrophils (Health Effects Institute 2001). Occupational exposure to rare earth metals, of which cerium is the major component, has been shown to induce rare earth pneumoconiosis with pathologic features of granulomas and interstitial fibrosis (Sabbioni et al. 1982; Waring and Watling 1990; McDonald et al. 1995). Pairon et al. (1994) have reported that in exposed individuals particles containing cerium were detected in the bronchoalveolar lavage (BAL) fluid and lung tissues even 20 years after the exposure stopped. Cerium is also linked to fibrosis of the heart, and CeO_2 is known to induce myocardial fibroblast proliferation and collagen deposition in rats (Prakash and Shivakumar 1998). These studies show that fibrosis, a crippling disease with no known effective treatment, may be a serious consequence of CeO_2 exposure. DEP, on the other hand, are known to induce changes in pulmonary immune/

Correspondence: Dr Jane Y. C. Ma, PhD, PPRB/HELD, NIOSH, 1095 Willowdale Road, Morgantown, West Virginia 26505-2888, USA. Tel: +1 304 285 5844. Fax: +1 304 285 5938. E-mail: jym1@cdc.gov

ISSN 1743-5390 print/ISSN 1743-5404 online © 2010 Informa UK, Ltd.
DOI: 10.3109/17435390.2010.519835

inflammatory responses that weaken innate and cell-mediated immunity (Yin et al. 2004). Thus, it is possible that the presence of CeO_2 in diesel exhaust emissions may modify DEP-induced lung inflammation and injury including oxidant generation, mitochondrial damage and apoptosis. The balance between pro- and anti-inflammatory cytokine productions by AM may impair host defense capability and weaken immunity. Thus CeO_2 exposure may elicit new disease states or add to DEP toxicity. The safety of CeO_2 has not been established, and the potential effects of CeO_2 in the diesel exhaust on the induction of pulmonary injury further underscores the need for detailed understanding of the health risks posed by cerium-containing diesel fuel in various occupational and environmental settings.

Alveolar macrophages (AM) are the principal cell type that mediates the pulmonary immune/inflammatory responses against inhaled particles, chemicals, or microorganisms. There is increasing evidence that AM exist in two functionally distinct populations, classically activated AM (M1) and alternatively activated AM (M2). M1 are known to orchestrate the inflammatory responses and are induced through Th1 cytokines (MacMicking et al. 1997; Hibbs 2002), whereas M2 are induced through either phagocytosis of apoptotic cells (Fadok et al. 1998) or by Th2 cytokine-mediated monocyte differentiation (Goerdt and Orfanos 1999). M1 cells metabolize L-arginine to L-citrulline through inducible nitric oxide synthase (iNOS) and generate nitric oxide that plays an important role in the induction of oxidative stress. In contrast, M2 cells produce L-ornithine through arginase-1 (Arg-1) leading to L-proline synthesis that may play a possible role in collagen deposition resulting in fibrosis (Shearer et al. 1997). This subset switching in AM has been reported in silica – and bleomycin-induced pulmonary fibrosis (Nau et al. 1997; Takahashi et al. 2001). Therefore, the differential activation of M1 or M2 may play a critical role in the pathogenesis of particle-induced lung injury.

Particle-induced pulmonary inflammation through reactive oxygen species generation (ROS), cytokine production via various signal transduction pathways, and transcriptional activation has been studied extensively. However, the involvement of down-regulation of these activation pathways in the pathogenesis of related lung disease has received much less attention. Osteopontin (OPN) is a multifunctional molecule highly expressed in chronic inflammatory and autoimmune diseases (Scatena et al. 2007). OPN secreted by AM has been shown to induce fibroblast proliferation and accumulate in bleomycin- and silica-induced animal models of pulmonary fibrosis (Nau et al. 1997; Takahashi et al. 2001). OPN production by alveolar epithelial cells has been demonstrated in human subjects with idiopathic pulmonary fibrosis (Pardo et al. 2005). Another anti-inflammatory protein, suppressor of cytokine signaling-1 (SOCS-1), is an inhibitor of cytokine signaling involved in accelerated pulmonary fibrosis in both animals and human subjects (Nakashima et al. 2008). These studies suggest that both OPN and SOCS-1 may be involved in the pathogenesis of pulmonary inflammation and fibrosis.

Studies have demonstrated that DEP and the organic extract of DEP are capable to inducing cellular ROS release and damage to mitochondria in AM (Zhao et al. 2009), leading to apoptosis and lung injury. Several *in vitro* cell culture studies have shown that CeO_2 protects the cells from oxidative stress by suppresing ROS production and inducing cellular resistance to an exogenous source of oxidative stress (Tsai et al. 2007; Xia et al. 2008). These investigators further demonstrated that pre-incubation of cells with CeO_2 before challenging cells with an organic extract of DEP significantly reduced the DEP extract-mediated cellular toxicity and oxidant generation, suggesting that CeO_2 has antioxidant activity.

To date, the potential effects of CeO_2 on oxidative stress, inflammation and injury of the lungs after *in vivo* exposure have not been characterized. The objective of the current study was to expose rats to CeO_2 by a single intratracheal instillation and to characterize CeO_2-induced pulmonary inflammation and injury, including the effects on AM functional changes. Specifically, this study investigated the particle-induced cellular generation of ROS, apoptosis, and functional modification of AM in the secretion of inflammatory and fibrogenic mediators in relation to lung toxicity in a rat model.

Methods

Particle characterization

Cerium oxide nanoparticles, 10 wt % in water with average diameter at ~20 nm, were obtained from Sigma-Aldrich (St Louis, MO, USA). CeO_2 samples diluted in saline were used for animal exposures. Since the CeO_2 nanoparticles form agglomerates in suspension, the size distribution of the agglomerates of CeO_2 was analyzed using dynamic light scattering (Nanotrac 252, Microtrac, Montgomeryville, PA, USA).

The CeO_2 suspension was analyzed using field scanning electron microscopy. Diluted particles suspensions were passed through a filter. After sputter coating, the specimens were examined with a Hitachi

Model S-4800 Field Emission Scanning electron microscope (Schaumburg, IL, USA) between 5 and 20 kV. In addition, the particles were diluted in double distilled filtered water and a drop was placed on a formvar-coated copper grid to dry, and the samples were viewed on a JEOL 1220 transmission electron microscope (Tokyo, Japan). Preliminary studies showed that unlike LPS the CeO_2 sample used in this study had no effect on *in vitro* AM cytokine production and was, therefore, assumed to be free of LPS contamination.

Animal exposures

Specific pathogen-free male Sprague-Dawley (Hla: SD-CVF) rats (6 weeks old) were purchased from Hilltop Laboratories (Scottdale, PA, USA). Rats were kept in cages individually ventilated with HEPA-filtered air, housed in an animal facility accredited by the American Association for Accreditation of Laboratory Animal Care. All rats were exposed and euthanized according to a standardized experimental protocol that complied with the Guidelines for the Care and Use of Laboratory Animals and was approved by the National Institute for Occupational Safety and Health Animal Care and Use Committee. The animals were humanely treated and with regard for alleviation of suffering. Animals were used after a one-week acclimatization period. For CeO_2 exposure, rats were anesthetized with sodium methohexital (35 mg/kg, i.p.) and placed on an inclined restraint board. Rats were exposed to 0.3 ml suspensions of CeO_2 for a final concentration of 0.15, 0.5, 1, 3.5 or 7 mg/kg body weight via a single intratracheal instillation. Saline (0.9% NaCl) was administered to control rats. The treated animals (at least six in each treatment group) were sacrificed at 1-, 10- or 28-day post-exposure.

The intratracheal instillation method used in this study was reported by an expert panel to be a useful method for screening the potential toxicity of a test material in the lower respiratory tract or for dose finding (Driscoll et al. 2000). They also reported that particular delivered at <100 mg by intratracheal instillation are cleared at a similar rate as would occur following inhalation. Thus, this exposure procedure has been chosen for the present study.

Isolation of bronchoalveolar lavage fluid and AM, and AM culture protocol

Animals were anesthetized with sodium pentobarbital (0.2 g/kg, i.p.) and exsanguinated by cutting the renal artery. AM were obtained by bronchoalveolar lavage (BAL) with a Ca^{++}, Mg^{++}-free phosphate-buffered medium (145 mM NaCl, 5 mM KCl, 1.9 mM NaH_2PO_4, 9.35 mM Na_2HPO_4, and 5.5 mM glucose; pH 7.4) as described previously (Yang et al. 2001). Briefly, the lungs were lavaged with 6 ml Ca^{++}, Mg^{++}-free phosphate-buffered medium for the first lavage, and subsequently lavaged with 8 ml of the same buffer for total 10 times or when ~total 80 ml BAL fluid were collected from each rat. The acellular supernate from the first lavage was saved separately from subsequent lavages for analysis of LDH activity and protein content. Cell pellets from each animal were centrifuged and combined, washed, and resuspended in a HEPES-buffered medium (145 mM NaCl, 5 mM KCl, 10 mM HEPES, 5.5 mM glucose, and 1.0 mM $CaCl_2$; pH 7.4). Cell counts and purity were measured using an electronic cell counter equipped with a cell sizing attachment (Coulter model Multisizer II with a 256C channelizer; Beckman Coulter, Fullerton, CA, USA).

AM-enriched cells were obtained by adherence of lavaged cells to a tissue culture plate as described previously (Yang et al. 1999) and cultured in fresh Eagle minimum essential medium (Lonza BioWhittaker, Walkersville, MD, USA) for an additional 24 h. AM-conditioned media were collected and centrifuged, and the supernates were saved in aliquots at -80^{o}C for further analysis of cytokines.

Lactate dehydrogenase (LDH), albumin content and chemiluminescence (CL)

The acellular LDH activity in the first BAL fluid was measured in fresh, unfrozen samples using Roche Diagnostic reagents and procedures (Roche Diagnostic Systems, Indianapolis, IN, USA), on an automated Cobas MIRA PLUS analyzer (Roche Diagnostic Systems). The albumin content in the first BAL fluid was measured based on albumin binding to bromcresol green with Sigma Diagnostic reagents and procedures following the manufacturer's protocol.

Luminol-dependent CL, a measure of ROS formation, was monitored using a Berthold LB953 Luminometer (Berthold, Wildbad, Germany). CL generated by BAL cells (1×10^6 AM/ml), was measured before and after stimulation with unopsonized zymosan (2 mg/ml final concentration; Sigma Chemical Company, St Louis, MO, USA), a particle stimulant that stimulates macrophages. The results were presented as total counts/15 min/10^6 AM. Zymosan-stimulated CL was calculated as the

total counts in the presence of stimulant minus the corresponding basal counts as described by Yang et al. (2001).

Confocal microscopic analysis of particle adhesion and/or uptake, intracellular ROS generation, and mitochondrial membrane potential.

AM isolated from CeO_2-exposed animals were adhered onto glass cover slip. Briefly, AM were plated in a 24-well tissue culture plate on glass coverslips that was pretreated for 1 h at 37°C with EMEM with 10% FBS to allow cell attachment, then washed with PBS once. The interaction of fluorescent beads with AM was determined using carboxylate-modified, yellow/green FluoSpheres (2.0 μm, at 30 beads/cell). AM were rocked at 37°C for 1 h, washed twice with PBS to remove any free beads, fixed with 10% formalin for 30 min, and stained with 0.1 μg/ml of fluorochrome Nile red (Molecular Probes) for 5 min. The glass coverslips were mounted on microscope slides, and images were recorded using confocal microscopy. The number of yellow fluorescent beads associated with AM indicates the particle adhesion and/or uptake by the cell.

The intracellular ROS production was monitored using dihydroethidium (DHE, Ex 518 nm, Em 605 nm). Mito Tracker Red CMXRos (Ex 579 nm, Em 599 nm) was used to detect the change of mitochondrial membrane potential. AM were adhered onto glass cover slip as described above, then incubated with DHE (5 μM) or with Mito Tracker Red (200 nM) for 15 or 30 min, respectively, washed with PBS and fixed with 10% buffered formalin phosphate for 10 min, and mounted on glass slides using Prolong Antifade (Invitrogen). Slides were imaged using a Zeiss LSM 510 confocal microscope (Carl Zeiss, Inc., Thornwood, NY, USA) at a 512 × 512 pixel size with a 40× water immersion objective for DHE or at 1024 × 1024 pixel size with a 100× oil immersion objective for Mito Tracker Red. The fluorescent intensity was used as measure of the ROS generation or mitochondrial membrane potential change.

NO production and cytokine assays

NO production was determined in AM-conditioned medium using the Greiss reaction (Green et al. 1982). IL-12 in AM-conditioned media was determined using enzyme-linked immunosorbent assays (ELISA) (Biosource International, Inc., Camarillo, CA, USA) according to the manufacturer's protocol. NO and IL-12 production by AM was also evaluated following *ex vivo* treatment with lipopolysacchride (LPS, 0.1 μg/ml).

Apoptosis assay and caspase 3/7 and 9 activities in AM

Apoptosis of AM was determined by measuring the levels of cytosolic histone-bound DNA fragments using a cell death ELISA kit (Roche Diagnostics Corp), according to the protocol provided by the manufacturer. The activities of caspase 3 and 9 were determined using Caspase-Glo 3/7 and Caspase-Glo 9 systems, respectively, according to the manufacturer's protocols (Promega, Madison, WI, USA).

Measurement of total phospholipids

The amount of total phospholipids in BAL fluid was measured as the phosphorus present in the lipid extracts, which were obtained using chloroform-methanol (2:1, v/v) as described previously (Bartlett 1959). Phospholipid content was obtained by multiplying lipid phosphorus values by 25 (Oyarzun and Clements 1978).

Comet assay

The comet assay was performed according to the manufacturer's instructions using a Comet Assay kit (Trevigen, Gaithersburg, MD, USA) under alkaline conditions. The slides were stained with SYBR green dye and comets were visualized and photographed at 200× magnification using a fluorescence microscope (Olympus AX70, Center Valley, PA, USA) with an image capture system (SamplePCI, Compix Inc., Cranberry Township, PA, USA).

RNA isolation and quantitation of mRNA

RT/PCR: Total RNA from BAL cells (~2×10^6 cells) or lung tissues was isolated using RNAqueous™ -4PCR kits (Ambion, Austin, TX, USA). RNA (1–2 μg) after the DNAse I-treatment was reverse transcribed, using Superscript II (Life Technologies, Gaithersburg, MD, USA). The cDNA generated was diluted 1:100, and 15 μl was used to conduct the PCR reaction according to the TaqMan® Master mix PCR kit instructions. The primers were selected from The Universal Probe Library (Roche Diagnostic Corp, Indianapolis, IN, USA). The primers and probes used are: Arginase-1 (BC091158) Probe Nos. 71: Sense – TGT GGG AAA AGC CAA TGA AC; Xsense – GAG ATG CTT CCA ATT GCC ATA. Collagen 1 (NM_053304) 67: Sense – GTG GAC AGG CTG GTG TGA T; Xsense – GGG ACA CCT

CGT TCT CCA G. Collagen 3 NM_032085) 64 : Sense – TGG ACC CCA AGG TCT TCC ; Xsense – CAT CTG ATC CAG GGT TTC CA. NFkB – (p50 subunit) (ENSRNOT 00000036838) Probe No. 25: Sense – CCC ACT TGC TGC CTC TCT; Xsense – GTC ACA CAC GCT GTC ATT ATC TC. Osteopontin (M14656) 41: Sense – GAG TTT GGC AGC TCA GAG GA; Xsense – TCT GCT TCT GAG ATG GGT CA. TGF-β1 (AY550025) 1: Sense – GGA AAG GGC TCA ACA CCT G; xsense – CAC AGC AGT TCT TCT CTG TGG A. SOCS-1 AJ243123.1|AJ243123:EMBL|: Probe # 20: Sense – GTC GGA GGG AGT GGG TGT; Xsense – CGA GAG GCG GGA TAA GGT. The comparative C_T (threshold cycle) method was used to calculate the relative concentrations (User Bulletin #2, ABI PRISM® 7700 Sequence Detector, PE Applied Biosystems, Foster City, CA, USA). Briefly, the method involves obtaining the C_T values for the cytokine of interest, normalizing to a reference gene (GAPDH in the present case), and deriving the fold increase compared to control.

Transmission electron microscope (TEM)

For AM ultrastructure analysis by TEM, cell pellets of BAL cells were fixed in Karnovsky's fixative (2.5% glutaraldehyde, 3.5% paraformaldehyde in 0.1 M Sodium Cacodylate buffer), pelleted, then embeded in 4% agarose and refixed for 2 h. The samples were post-fixed in 1% osmium tetroxide (120 min at 4°C), mordanted in 1% tannic acid (pH 7.0) and block stained in 0.5% uranyl acetate (both at room temperature for 60 min) all in a buffer of 8% sucrose and 0.9% sodium chloride. When the staining was complete, the solution was changed to 70% ethyl alcohol and then 90%, samples were then rinsed twice with 100% twice for 15 min each. Then placed into a solution of 1:1 100% ethyl alcohol to propylene oxide for 15 min, and finally into 100% propylene oxide changing the solution twice. The sample solution was replaced with a 1:1 of propylene oxide and LX112 embedding media, follow by a 3:1 solution for 30 min, and then finally into 100% solution of LX112 overnight on a rotating platform. This solution was changed again for an additional 4 h, then placed into embedding molds and placed into a 60°C oven for 48 h. Thick (0.5 μ) sections were cut and stained with a 1% toluidine blue (in 1% sodium borate) solution on a hot plate for 90 sec. Thin sections (70 nm) were placed on 200 mesh copper grids and stained with 4% aqueous uranyl acetate and Reynold's lead citrate for 15 and 20 min, respectively. Images were taken on a JEOL 1220 transmission electron microscope at 80 kV.

Histological examination

Rat lung tissues from different exposure groups were fixed immediately after sacrifice by intratracheal instillation of 10% neutral buffered formalin at a pressure of 30 cm H_2O (at an altitude of 960 ft), embedded in paraffin, and stained with hematoxylin and eosin for light microscopic examinations (Prophet et al. 1992).

Morphometric analysis of inflammatory cell response

Quantitative morphometric methods were used to measure the density of AM and polymorphonuclear leukocytes (PMN) in the alveolar region (Underwood 1970) as a measure of the inflammatory cell response. This consisted of basic point counting of Sirius Red/Mayer's hematoxylin stained sections of the lung to determine the fraction of the alveolar region volume occupied by AM and PMN. To accomplish this, volume density was determined from counting the number of points over AM and PMN in the section relative to total alveolar region points. The point count were made using a 121-point overlay graticule at 100× magnification taken at six locations equally spaced across each section (one section per animal). This process was repeated for two different sections for each animal. In order to limit the measurements to alveolar parenchyma, areas containing airways or blood vessels greater than 25 μm in diameter were excluded from the analysis. The alveolar region volume of AM and of PMN was computed from the ratio of points over AM and of PMN, respectively, to the total alveolar region points and divided by 100 to express the numbers as a percentage of the alveolar region volume.

Statistical analysis

Data are presented as means ± standard errors. Comparisons were made using analysis of variance (ANOVA) with means testing by Dunnett's test. A $p \leq 0.05$ was considered to be significant.

Results

The suspensions of CeO_2 nanoparticles used in this study were examined using dynamic light scattering, which indicates the presence of μm-sized agglomerates (Figure 1A). Field emission SEM and TEM micrographs of CeO_2 suspensions are shown in Figure 1B and 1C and confirm the presence

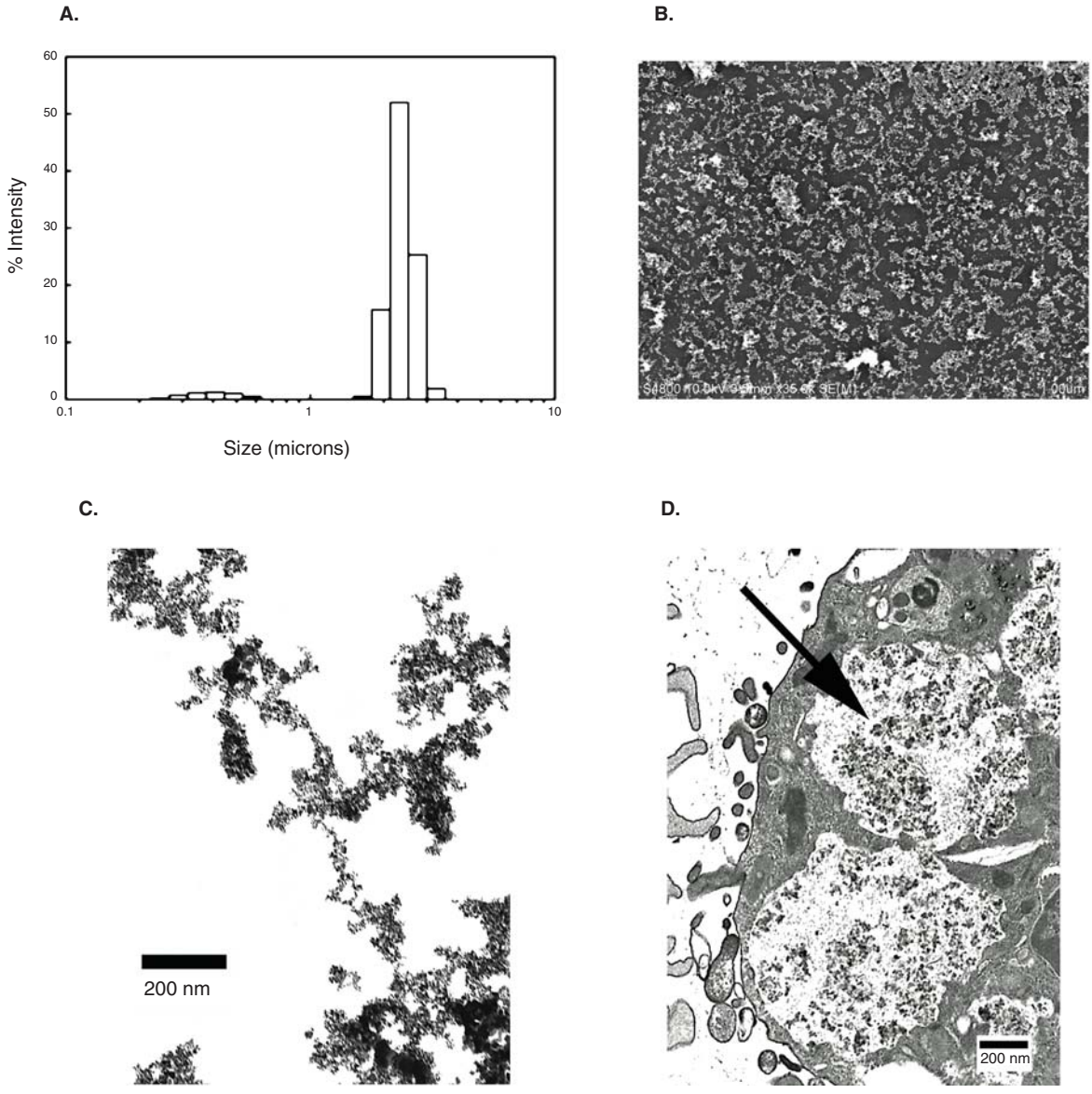

Figure 1. Characterization of a CeO_2 suspension and localization of CeO_2 particles in AM. (A) Dynamic light scattering. The % channel indicates the intensity of particles in each channel size. (B) Field emission SEM. (C) TEM micrograph of CeO_2 nanoparticles prepared from a dilute suspension (scale bar = 200 nm). (D) TEM micrograph of agglomerates of CeO_2 in AM. AM was isolated from CeO_2-exposed rats at 10 days post exposure (scale bar = 200 nm).

of agglomerated structures in suspension. A TEM micrograph of AM isolated by BAL from CeO_2 (3.5 mg/kg)-exposed rats at 10 days post exposure, shows the presence of sub-μm-sized CeO_2 particles within intracellular vesicles (Figure 1D).

Exposure of rats to CeO_2 (at dose of 0.15, 0.5, 1, 3.5 and 7 mg/kg) caused significant lung inflammation and toxicity to lung cells. The results show that the number of AM in the BAL fluid was not markedly altered at 1 day after exposure, but was significantly increased, in a dose-related manner, at 10 and 28 days post exposure, indicating that recruitment of AM occurred during the inflammatory state (Figure 2A). However, there was a significant recruitment of PMN at 1 day post exposure with a substantial, dose-dependent and persistent elevation of PMN through the 28 day post exposure time period (Figure 2B). Figure 2C shows a dose-dependent increase in leakage of cellular LDH into the airspace. Air/capillary damage, determined by elevated albumin content in the air space (Figure 2D), also persisted through 28 days after exposure. Thus, the results demonstrated that exposure of rats to CeO_2 caused significant and sustained lung inflammation, cytotoxicity and air/capillary barrier damage.

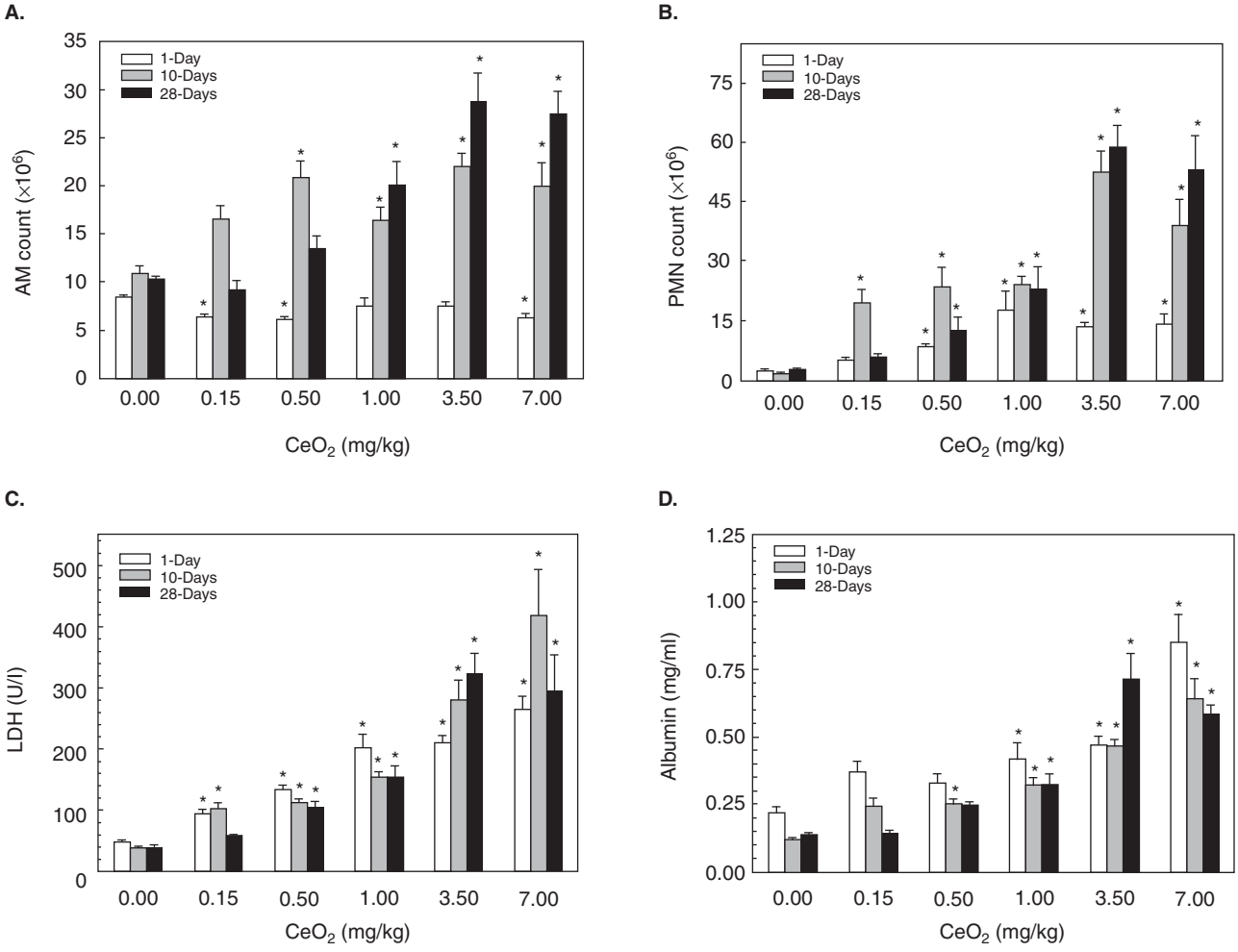

Figure 2. Effects of CeO_2 on lung inflammation and injury. AM (A), PMN infiltration (B) and LDH activity (C) and albumin content (D) in BAL fluid at 1, 10 and 28 days post-exposure. *Significantly different from saline control; $p \leq 0.05$.

Figure 3A shows a significant ROS released from CeO_2-exposed AM in response to *ex vivo* zymosan stimulation monitored by CL when compared to controls, suggesting CeO_2 markedly potentiated AM responsiveness. The activation noted at 1 day post exposure was significantly reduced but remained above the control level at 28 days post exposure. Activation of AM from CeO_2-exposed rats was also associated with increased adhesion and/or uptake of fluorescent beads by AM when compared to the controls as shown in Figure 3B, monitored using confocal microscopic analysis. To provide more insight into CeO_2-mediated intracellular events, the effect of CeO_2 exposure on intracellular ROS generation, mitochondrial function, and cell survival were examined. The results show that CeO_2 did not induce intracellular ROS generation (Figure 3C) or mitochondrial dysfunction (Figure 3D) in AM at 1 day post exposure, and these findings were sustained through 28 days-post exposure (data not shown). In addition, Figure 4A shows that *in vivo* CeO_2 induced apoptosis of AM at 1 day post-exposure. This CeO_2-induced apoptosis pathway is through the activation of caspase 9 (Figure 4B) and caspase 3 (Figure 4C). Studies using the comet assay indicated that exposure of rats to CeO_2 did not cause DNA damage in AM (data not shown).

The histological evaluation of particle-induced lung inflammation at 28 days after CeO_2 exposure demonstrated large, clumps of material in the alveolar space which were generally acellular (Figure 5A, open arrow). However, no granulomatous lesions were observed. Results from morphometric measurement of the total volume of AM and PMN in the lungs demonstrated that CeO_2 significantly elevated AM and PMN alveolar region volume in the lung when compared to the saline controls (Figure 5B). To further examine the acellular clumps of materials in the CeO_2-exposed AM, the phosphlipid (PL) content in the BAL fluid was examined. The results

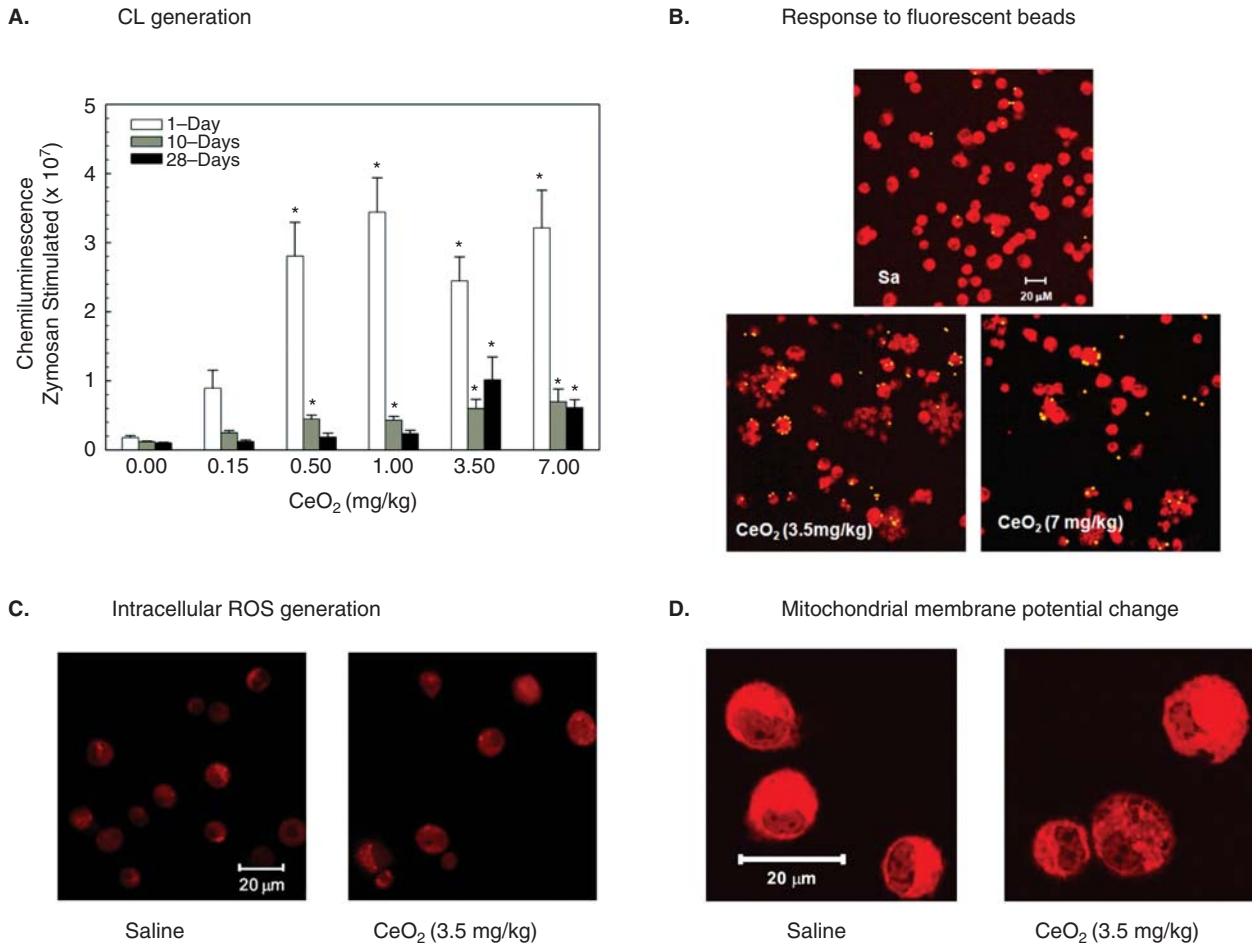

Figure 3. Effects of *in vivo* exposure to CeO_2 on AM function. Responses of AM, isolated from CeO_2-exposed rats to zymosan challenge in ROS production measured by CL (A). The attachment of fluorescent beads (yellow) to control- or CeO_2-exposed AM (scale bar = 20 μm) (B). Effects of CeO_2 exposure on intracellular ROS (C) and mitochondrial membrane potential change (D) were monitored at 1 day post exposure using confocal microscopic analysis (scale bar = 20 μm). *Significantly greater than saline control; $p \leq 0.05$.

show a significant increase of PL in BAL fluid from CeO_2-exposed compared to saline-exposed rats (Figure 5C). TEM analysis (Figure 5D) shows a significantly increased number of vesicles filled with surfactant material in AM and lamella bodies around AM obtained at 10 days post exposure. AM from control rats lack these lipid inclusions.

An examination of the effects of *in vivo* exposure to CeO_2 on the expression of selected genes, including nuclear factor (NF)-κB, OPN, TGF-β and SOCS1, in BAL cells showed that at 1 day post-exposure there was a significant induction of mRNA expression in BAL cells of NF-κB and SOCS1 in CeO_2 – compared to saline-exposed control rats (Figure 6A). The expression of OPN was not increased in BAL cells when compared to the control; however, it was significantly induced in CeO_2-exposed lung tissues (Figure 6B), suggesting activation of this multifunctional cytokine during inflammatory injury.

The potential functional change of AM from M1 to M2 was investigated. Figure 7A shows that at 1 day post exposure, NO production by AM was significantly elevated at 1 mg/kg CeO_2, while returning to the basal level at higher concentrations. It is possible that higher concentrations of CeO_2 scavenged NO due to the redox characteristics of this particle. CeO_2-exposed AM also exhibited significantly induced pro-inflammatory cytokine, IL-12, secretion (Figure 7B). In response to *ex vivo* LPS (0.1 μg/ml) challenge, CeO_2-exposed AM exhibited significantly attenuated LPS-induced NO production (Figure 7C), but markedly enhanced IL-12 production (Figure 7D).

At 28 days post-exposure, CeO_2-exposed AM no longer exhibited enhanced NO production (data not shown). Furthermore, mRNA expression of Arg-1 in CeO_2-exposed BAL cells was significantly increased at 28 days post-exposure (Figure 8A), suggesting that the particle exposure induced AM switching

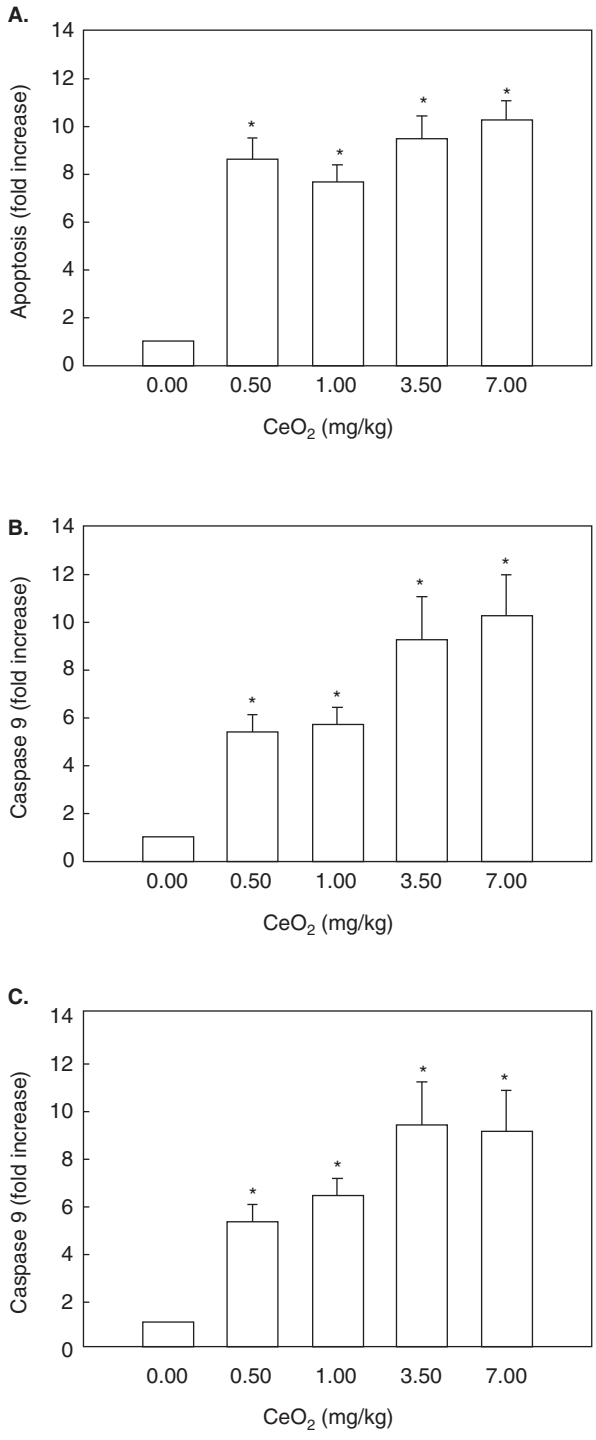

Figure 4. CeO_2 exposure induced apoptosis. AM, isolated from CeO_2-exposed rats at 1 day post-exposure, show increased apoptosis (A), caspase 9 (B) and 3 (C) in the AM cell culture, after a 24 h incubation period. *Significantly different from saline control; $p \leq 0.05$.

from classical inflammatory M1 to fibrogenic M2 subsets. The induction of OPN mRNA, at 1 and 28 days post CeO_2 exposure was also elevated in lung tissue in a time-dependent manner (Figure 8B).

Discussion

We have established through cellular measurements and histological examinations that CeO_2 induces a significant pulmonary inflammatory

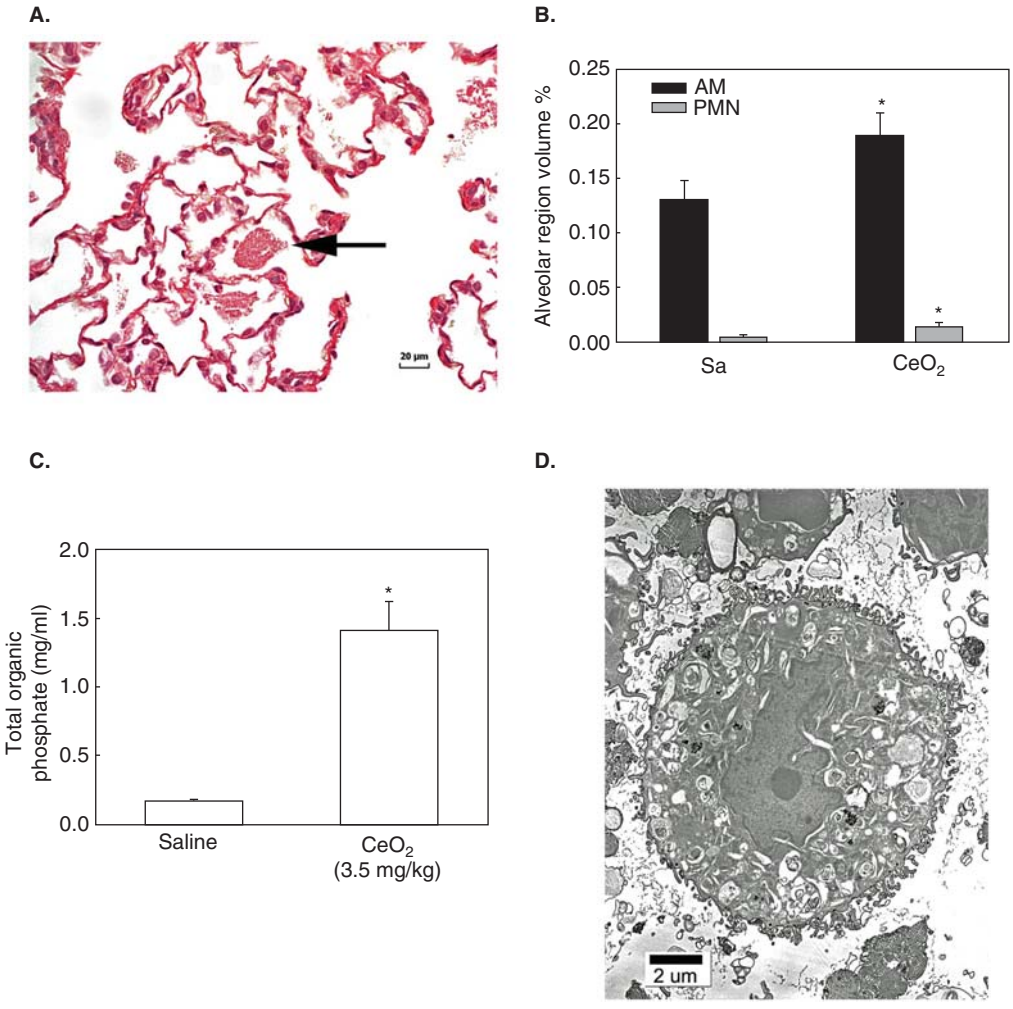

Figure 5. Exposure of rats to a single intratracheal instillation of CeO_2-induced lung lipidosis at 28 days after exposure. Light micrograph lung tissues, produce large, sometimes alveolar sized, clumps of material in the airspace which were generally acellular and rich in surfactant and tubular myelin (arrow, scale bar = 20 µm) (A). The cellular volume of AM and PMN expressed as a percentage of the alveolar region volume in the saline or CeO_2-exposed lungs isolated at 28 days after exposure were determined using quantitative morphometric measurements (B). Phospholipids content in the BAL fluid collected from CeO_2-exposed rat at 28 days post-exposure (C). TEM of an AM harvested from a CeO_2-exposed rat at 10 days post-exposure (D). *Significantly different from saline control; $p \leq 0.05$.

response that leads to lung injury and alteration of AM inflammatory activities. The inflammatory response was evidenced by delayed increase in AM and the rapid and sustained infiltration of PMN into the alveolar space, while lung injury was noted by leakage of LDH and albumin from cells and pulmonary capillary vessels, respectively. The histological evidence showed that AM in CeO_2-exposed lungs were significantly enlarged due to the accumulation of particles and excessive production of surfactant materials, leading to phospholipidosis. In addition, the histological examination showed that exposure of rats to CeO_2 for four weeks did not cause granulomatous lesions in the lung tissue, but there was an extended inflammation characterized by a significant elevation of AM and PMN alveolar volume in the lung parenchyma as judged by quantitative morphometric measurement. These results further demonstrated that exposure of rats to CeO_2 by intratracheal instillation caused a significant lung response.

The results also show that CeO_2 significantly induced cellular activity and oxidative responses and apoptosis. At 1 day post exposure, CeO_2 exposure resulted in dose-dependent increase in the attachment of particles to AM, and enhanced ROS release by AM in response to zymosan stimulation. On the other hand, CeO_2 did not induce intracellular ROS release or alter mitochondrial potential, yet it induced apoptosis through activation of caspase 9 and caspase 3. These findings indicate that CeO_2 exposure can alter AM function. In contrast, our previous studies have shown that DEP exposure significantly

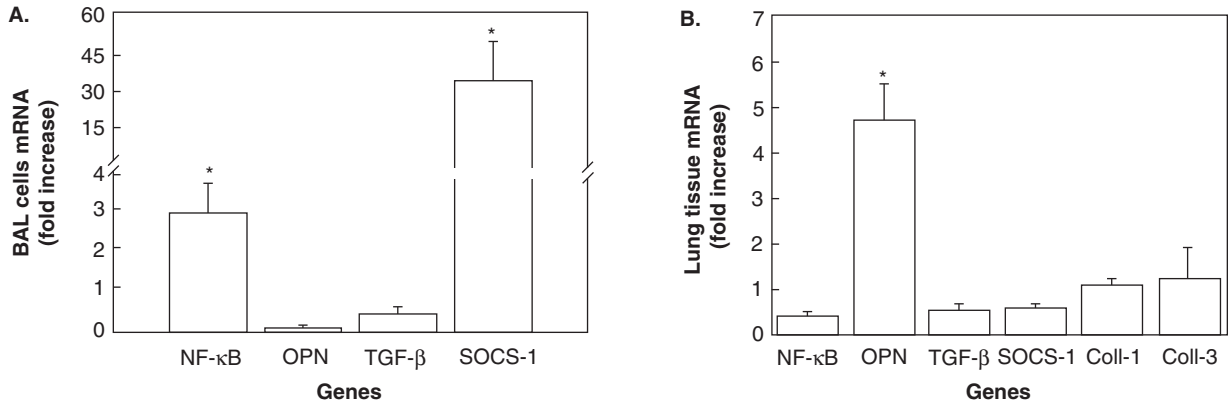

Figure 6. Selected mRNA gene expressions in AM and lung tissue. mRNA expression were determined in AM and lung tissue, collected from rats at 1 day after exposed to saline, or CeO_2 (3.5 mg/kg). *Significantly different from saline control; $p \leq 0.05$.

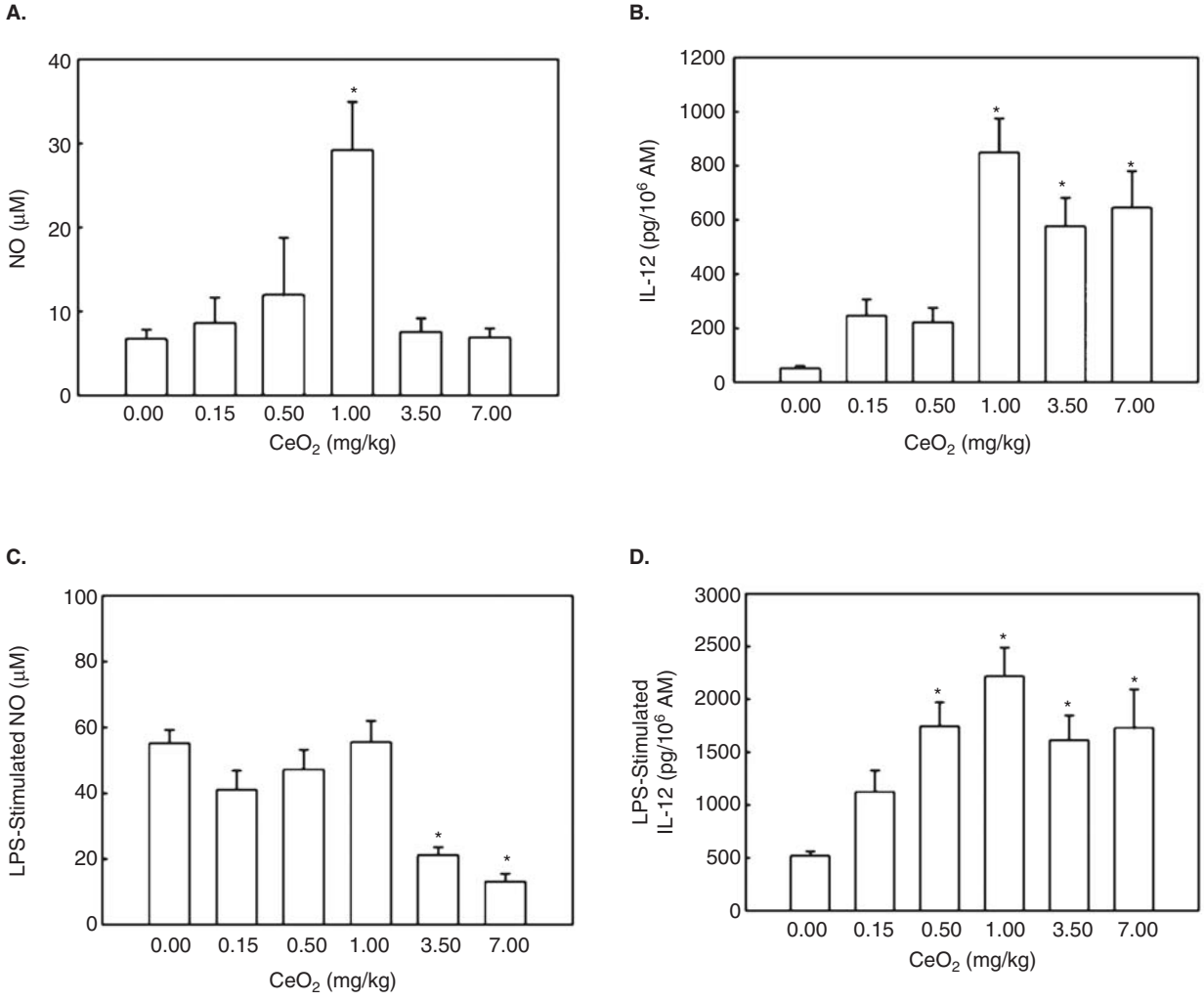

Figure 7. Effects of CeO_2 exposure on NO and IL-12 production by AM isolated at 1 day post exposure. AM were obtained by BAL and cultured for 24 h as described in *Methods*. The supernates were collected and analyzed for production of NO (A) and IL-12 (B) secreted in the AM culture medium. The production of NO and IL-12 in response to *ex vivo* LPS (0.1 μg/ml) challenge were presented in C and D, respectively. *Significantly different from saline control; $p \leq 0.05$.

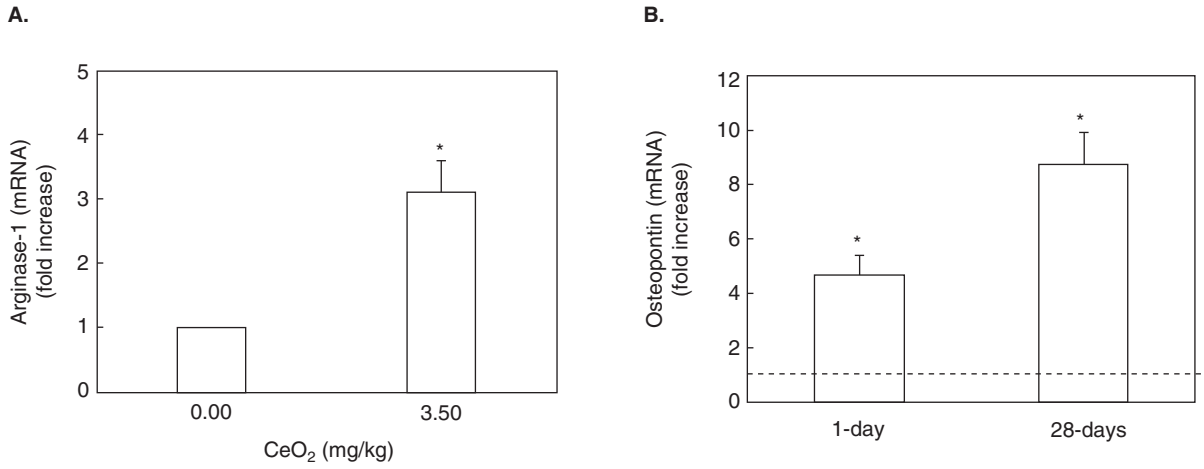

Figure 8. mRNA expression of Arg-1 and OPN. The mRNA of Arg-1 in BAL cells isolated from saline or CeO_2 (3.5 mg/kg) at 28 days post exposure (A). OPN mRNA expression in the lung tissues isolated from rats exposed to saline or CeO_2 (3.5 mg/kg) at 1 and 28 days post exposure (The dash line represents the control). *Significantly different from saline control; $p \leq 0.05$.

induced intracellular ROS production and mitochondrial damage in AM and promoted apoptosis through a pathway involving cytochrome c release from mitochondria (Zhao et al. 2009). These findings suggest that the presence of CeO_2 in the diesel exhaust may alter DEP-induced lung toxicity. These results warrant further investigations, which are currently being conducted in our laboratory.

At the present time, the pulmonary cellular responses to *in vivo* CeO_2 exposure have not been fully investigated. Studies using cell lines in culture have demonstrated that CeO_2 was taken up into cellular compartments without cytotoxicity. CeO_2 also suppressed ROS production and induced cellular resistance to an exogenous source of oxidative stress (Xia et al. 2008). CeO_2 has also been shown to exhibit cardio-protective effects in animal models after intravenous administration (Niu et al. 2007), suggesting that CeO_2 attenuated myocardial oxidative stress and inflammatory processes through their auto-regenerative antioxidant properties. The present study shows that CeO_2 exposure induced cytotoxicity and damage to the air/capillary barrier at 1 day after exposure, which was sustained throughout 28 days exposure time period. Zymosan-stimulated oxidant generation by CeO_2-exposed AM at 28 days post-exposure, although less than at 1 day, was still markedly higher than the controls, suggesting that CeO_2-induced oxidant release by AM may be related to lung cell toxicity and injury in the animal model. At 1 day post CeO_2 exposure, AM showed increased IL-12 secretion and an apoptotic response. These results indicate that CeO_2 activates the inflammatory AM, M1, responsible for the lung inflammation in acute exposure. However, the lungs also responded with a self-defense mechanism initiated through the induction of SOCS-1 by lung cells. This induction of SOCS-1 suggests that the particle-induced inflammatory response may trigger attempted self-defense mechanism(s) by AM to decrease further activation by inflammatory stimuli. SOCS-1 has been shown to negatively regulate IFN-γ-mediated immune/inflammatory responses (Yoshimura et al. 2003) and to play a role in pulmonary inflammation and fibrosis (Shoda et al. 2007; Nakashima et al. 2008). It is likely that the balance of SOCS-1, IL-12 and other mediators would affect the final outcome of lung injury or recovery.

At 28 days after CeO_2 exposure, there was an increased expression of Arg-1 in lung cells. The induction of Arg-1 is a marker for phenotype switching of AM from M1 to M2. The metabolism of L-Arg to orthonine leads to proline formation and subsequent usage in collagen synthesis, which may play a role in the development of lung fibrosis (Munder et al. 1998). In addition, CeO_2 also induced OPN mRNA expression in lung tissue through out the 28-day exposure period in this study. This may also lead to pulmonary fibrosis. There is increasing evidence that OPN is an important mediator of the pulmonary fibrotic response, since it has been shown to work in concert with PDGF to induce fibroblast proliferation and is required for TGF-β1-mediated myofibroblast differentiation (Lenga et al. 2008), leading to the development of lung fibrosis. OPN has also been shown to accumulate in the regions of bleomycin- and silica-induced lung fibrosis in animal models (Nau et al. 1997; Takahashi et al. 2001). The role of a functional change of AM and/or the accumulation of surfactant material as evidenced by

phospholipidosis in the lung and accumulated surfactant materials in vacuoles in initiation and progression of pulmonary fibrosis is under investigation in our laboratory.

The projected human pulmonary dose for inhalation of CeO_2 in diesel exhaust from engines using a CeO_2 fuel additive is 0.09 μg/kg body weight for 8 h (Health Effects Institute [HEI] 2001). CeO_2 is insoluble particle, and studies have shown that the clearance of CeO_2 from the lung may take 20 years or more (Pairon et al. 1994). As a diesel exhaust product, it is likely that the potential exposure (occupational or environmental) to CeO_2 is continuous and the lung burden is cumulative. Assuming a person has been exposed to the projected dose for 40 years with 8 h working day, the total lung burden of CeO_2 will be 936 μg/kg (0.09 μg/kg.d × 5 d/week × 52 week/year × 40 years = 936 μg/kg). Usually, conversion from rodents to humans includes a safety factor of 10-fold. Therefore, it is not unreasonable then, to assess the potential toxicological consequence from the exposure to CeO_2 at 150 μg/kg to 7 mg/kg body weight, as done in this study.

However, when CeO_2 used as diesel fuel catalyst, CeO_2 and DEP co-exist in the diesel exhaust emissions. Studies have shown that exposure of animals to DEP mediated Th2 immune response (Yin et al. 2007), Th2 cytokines are known to play important role in mediating M2 induction (Goerdt and Orfanos 1999). These Th2 cytokines produced in the animals exposed to both CeO_2 and DEP may modify resultant lung toxicity. Thus, the cooperative effects between CeO_2 and DEP on lung toxicity also require in depth investigation.

In summary, our studies show that CeO_2 nanoparticles cause dose-dependent inflammation and lung injury that includes sustained LDH leakage into the airspaces, recruitment of PMN and AM to the injury site, and apoptosis of AM. CeO_2-induced AM apoptosis involves activation of caspases 9 and 3, but is independent of mitochondrial release of cytochrome c. AM obtained from CeO_2-exposed rats (1 day) showed stimulated production of IL-12 and augmented ROS generation in response to zymosan challenge. SOCS-1 was also induced and may negatively regulate CeO_2-induced inflammatory responses in the lung. The mRNA for Arg-1 was induced significantly after 28 days post CeO_2 exposure, indicating that there may be a switch of AM from the inflammatory M1 to the fibrogenic M2 subset. The CeO_2 exposure was also associated with increased expression of OPN in lung tissue through 28 days post-exposure. OPN has been shown to protect cells from cell death by promoting a fibrogenic response. Therefore, the present studies shows that exposure of rats to CeO_2 resulted in significant lung responses, including lung inflammation, cytotoxicity, lung injury, AM functional changes, induction of phospholipidosis, and release of pro-inflammatory and fibrotic cytokines. These results suggest that the use of cerium compounds in diesel fuel, which results in the emission of mixed CeO_2 and DEP nanoparticles, may pose a serious health risk, and further investigation is warranted.

Disclaimer

The findings and conclusions in this manuscript have not been formally disseminated by the National Institute for Occupational Safety and Health and should not be construed to represent any agency determination or policy.

Declaration of interest: The authors report no conflicts of interest. The authors alone are responsible for the content and writing of the paper.

References

Bartlett GR. 1959. Phosphorus assay in column chromatography. J Biol Chem 234:466–468.

Czerwinski J, Napoli S, Compte P, Matter U, Mosimann T. 2000. Investigations with the Corning-diesel particulate filter and cerium-additive Eolys DPX 9 on the Liebherr D914T engine. VERT report. Technik Thermiche Maschinen, Niwderrohrdorf, Switzerland.

Dong CC, Yin XJ, Ma JYC, Millecchia L, Barger MW, Roberts JR, Zhang ZD, Antonini JM, Dey RD, Ma JKH. 2005. Exposure of Brown Norway rats to diesel exhaust particles prior to ovalbumin (OVA) sensitization elicits IgE adjuvant activity but attenuates OVA-induced airway inflammation. Toxicol Sci 88:150–160.

Driscoll KE, Driscoll KE, Costa DL, Hatch G, Henderson R, Oberdörster G, Salem H, Schlesinger RB. 2000. Intratracheal instillation as an exposure technique for the evaluation of respiratory tract toxicity: Uses and limitations. Toxicol Sci 55:24–35.

Fadok VA, Bratton DL, Konowal A, Freed PW, Westcott JY, Henson PM. 1998. Macrophages that have ingested apoptotic cells in vitro inhibit proinflammatory cytokine production through autocrine/paracrine mechanisms involving TGF-beta, PGE2, and PAF. J Clin Invest 101:890–898.

Goerdt S, Orfanos CE. 1999. Other functions, other genes: Alternative activation of antigen-presenting cells. Immunity 10: 137–142.

Green LC, Wagner DA, Glogowski J, Skipper PL, Wishnok JS, Tannenbaum SR. 1982. Analysis of nitrate, nitrite, and [15N] nitrate in biological fluids. Anal Biochem 126:131–138.

Heeb NV. 1998. Influence of particulate trap systems on the composition of diesel engine exhaust gas emissions (Part II). EMPA Research Report 112847. Swiss Federal Laboratories for Materials Testing and Research, Dubendorf, Switzerland.

Health Effects Institute (HEI). 2001. Evaluation of human health risk from cerium added to diesel fuel. In: Hibbs JB Jr, editor. HEI Communication 9, Boston, MA, USA. Integrated

Laboratory Systems. 2002. Infection and nitric oxide. J Infect Dis 185(Suppl. 1):S9–17.

Lenga Y, Koh A, Perera AS, McCulloch CA, Sodek J, Zohar R. 2008. Osteopontin expression is required for myofibroblast differentiation. Circ Res 102:319–327.

MacMicking J, Xie QW, Nathan C. 1997. Nitric oxide and macrophage function. Annu Rev Immunol 15:323–350.

McDonald JW, Ghio AJ, Sheehan CE, Bernhardt PF, Roggli VL. 1995. Rare earth (cerium oxide) pneumoconiosis: Analytical scanning electron microscopy and literature review. Mod Pathol 8:859–865.

Munder M, Eichmann K, Modolell M. 1998. Alternative metabolic states in murine macrophages reflected by the nitric oxide synthase/arginase balance: Competitive regulation by CD4+ T cells correlates with Th1/Th2 phenotype. J Immunol 160: 5347–5354.

Nakashima T, Yokoyama A, Onari Y, Shoda H, Haruta Y, Hattori N, Naka T, Kohno N. 2008. Suppressor of cytokine signaling 1 inhibits pulmonary inflammation and fibrosis. J Allergy Clin Immunol 121(5):1269–1276.

Nau GJ, Guilfoile P, Chupp GL, Berman JS, Kim SJ, Kornfeld H, Young RA. 1997. A chemoattractant cytokine associated with granulomas in tuberculosis and silicosis. Proc Natl Acad Sci USA 94:6414–6419.

Niu J, Azfer A, Rogers LM, Wang X, Kolattukudy PE. 2007. Cardioprotective effects of cerium oxide nanoparticles in a transgenic murine model of cardiomyopathy. Cardiovasc Res 73:549–559.

Oyarzun MJ, Clements JA. 1978. Control of lung surfactant by ventilation, adrenergic mediators, and prostaglandins in the rabbit. Am Rev Respir Dis 117:879–891.

Pairon JC, Roos F, Iwatsubo Y, Janson X, Billon-Galland MA, Bignon J, Brochard P. 1994. Lung retention of cerium in humans. Occup Environ Med 51:195–199.

Pardo A, Gibson K, Cisneros J, Richards TJ, Yang Y, Becerril C, Yousem S, Herrera I, Ruiz V, Selman M, Kaminski N. 2005. Up-regulation and profibrotic role of osteopontin in human idiopathic pulmonary fibrosis. PLoS Med 2:e251.

Prakash KB, Shivakumar K. 1998. Alterations in collagen metabolism and increased fibroproliferation in the heart in cerium-treated rats: Implications for the pathogenesis of endomyocardial fibrosis. Biol Trace Elem Res 63:73–79.

Prophet EB, Mills B, Arrington JB, Sobin LH, editors. 1992. In: Laboratory methods histotechnology. Washington, DC: Armed Forces Institute of Pathology. pp 1–279.

Sabbioni E, Pietra R, Gaglione P, Vocaturo G, Colombo F, Zanoni M, Rodi F. 1982. Long-term occupational risk of rare-earth pneumoconiosis. A case report as investigated by neutron activation analysis. Sci Total Environ 26:19–32.

Scatena M, Liaw L, Giachelli CM. 2007. Osteopontin: A multifunctional molecule regulating chronic inflammation and vascular disease. Arterioscler Thromb Vasc Biol 27:2302.

Shearer JD, Richards JR, Mills CD, Caldwell MD. 1997. Differential regulation of macrophage arginine metabolism: A proposed role in wound healing. Am J Physiol 272: E181–190.

Shoda H, Yokoyama A, Nishino R, Nakashima T, Ishikawa N, Haruta Y, Hattori N, Naka T, Kohno N. 2007. Overproduction of collagen and diminished SOCS1 expression are causally linked in fibroblasts from idiopathic pulmonary fibrosis. Biochem Biophys Res Commun 353:1004–1010.

Takahashi F, Takahashi K, Okazaki T, Maeda K, Ienaga H, Maeda M, Kon S, Uede T, Fukuchi Y. 2001. Role of osteopontin in the pathogenesis of bleomycin-induced pulmonary fibrosis. Am J Respir Cell Mol Biol 24:264–271.

Tsai YY, Oca-Cossio J, Agering K, Simpson NE, Atkinson MA, Wasserfall CH, Constantinidis I, Sigmund W. 2007. Novel synthesis of cerium oxide nanoparticles for free radical scavenging. Nanomedicine 2:325–332.

Underwood EE. 1970. Quantitative stereology. Reading, MA: Addison-Wesley.

Waring PM, Watling RJ. 1990. Rare earth deposits in a deceased movie projectionist. A new case of rare earth pneumoconiosis? Med J Aust 153:726–730.

Xia T, Kovochich M, Liong M, Madler L, Gilbert B, Shi H, Yeh JI, Zink JI, Nel AE. 2008. Comparison of the mechanism of toxicity of zinc oxide and cerium oxide nanoparticles based on dissolution and oxidative stress properties. ACS Nano 2: 2121–2134.

Yang HM, Antonini JM, Barger MW, Butterworth L, Roberts BR, Ma JK, Castranova V, Ma JY. 2001. Diesel exhaust particles suppress macrophage function and slow the pulmonary clearance of Listeria monocytogenes in rats. Environ Health Perspect 109:515–521.

Yang HM, Barger MW, Castranova V, Ma JK, Yang JJ, Ma JY. 1999. Effects of diesel exhaust particles (DEP), carbon black, and silica on macrophage responses to lipopolysaccharide: Evidence of DEP suppression of macrophage activity. J Toxicol Environ Health 58:261–278.

Yin XJ, Dong CC, Ma Jane YC, Roberts JR, Antonini JM, Ma JKH. 2007. Suppression of phagocytic and bactericidal functions of rat alveolar macrophages by the organic component of diesel exhaust particles. J Toxicol Environ Health Part A 70:820–828.

Yin XJ, Ma JY, Antonini JM, Castranova V, Ma JK. 2004. Roles of reactive oxygen species and heme oxygenase-1 in modulation of alveolar macrophage-mediated pulmonary immune responses to Listeria monocytogenes by diesel exhaust particles. Toxicol Sci 82:143–153.

Yoshimura A, Mori H, Ohishi M, Aki D, Hanada T. 2003. Negative regulation of cytokine signaling influences inflammation. Current Opin Immunol 15:704–708.

Zhao H, Ma JK, Barger MW, Mercer RR, Millecchia L, Schwegler-Berry D, Castranova V, Ma JY. 2009. Reactive oxygen species- and nitric oxide-mediated lung inflammation and mitochondrial dysfunction in wild-type and iNOS-deficient mice exposed to diesel exhaust particles. J Toxicol Environ Health A 72:560–570.